Imbibition dynamics of nano-particulate ink-jet drops on micro-porous media
Hsiao, W.-K., Hoath, S. D., Martin, G. D., Hutchings, I. M., Chilton, N. B. and Jones, S., Proc Nanotech 2011 Conference, Boston, June 2011.

Imbibition dynamics of nano-particulate ink-jet drops on micro-porous media

W.-K. Hsiao*, S. D. Hoath*, G. D. Martin*, I. M. Hutchings*, N. B. Chilton** and S. Jones**

*Department of Engineering, University of Cambridge
Cambridge CB3 0FS, United Kingdom, wkh26@cam.ac.uk
**Printed Electronics Ltd., Tamworth, United Kingdom, steve.jones@printedelectronics.co.uk

ABSTRACT

Ink-jet printing of nano-metallic colloidal fluids on to porous media such as coated papers has become a viable method to produce conductive tracks for low-cost, disposable printed electronic devices. However, the formation of well-defined and functional tracks on an absorbing surface is controlled by the drop imbibition dynamics in addition to the well-studied post-impact drop spreading behavior.

This study represents the first investigation of the real-time imbibition of ink-jet deposited nano-Cu colloid drops on to coated paper substrates. In addition, the same ink was deposited on to a non-porous polymer surface as a control substrate. By using high-speed video imaging to capture the deposition of ink-jet drops, the time-scales of drop spreading and imbibition were quantified and compared with model predictions. The influences of the coating pore size on the bulk absorption rate and nano-Cu particle distribution have also been studied.

Keywords: nano-copper colloid, imbibition, high-speed imaging, drop deposition, ink-jet

1 INTRODUCTION

While ink-jet printing is a mature technology in graphic arts applications, its application as a manufacturing process for depositing functional materials has also attracted significant interest in recent years. As a non-impact, additive and digital process, ink-jet printing is particularly suitable in manufacturing low-cost disposable printed electronic devices where functional materials often need to be applied to flexible substrates such as textiles and papers with low temperature-tolerance.

As the ink-jet printed patterns in electronic applications require functionalities such as electrical conduction, there is a greater demand for resolution and consistency. The basic principle of forming patterns by ink-jet printing is to deposit drops sequentially and allow them to consolidate on surfaces. Controlling the pattern features therefore requires a good understanding of ink drop deposition and spreading behavior on, in our case, absorbing surfaces. While the spreading dynamics of liquid drops on rigid, non-absorbent surfaces has been widely studied [1-5], the effect of liquid imbibition during spreading has received far less attention [6-9]. Furthermore, it is challenging to conduct experimental studies at the length and time scales of ink-jet printing. Only recently have advances in high-speed imaging enabled detailed study of the impact and spreading behavior of ink-jet drops from microseconds to seconds post-impact [10, 11]. However, to the best of the authors' knowledge, such investigations have yet to be extended to the case of ink-jet deposition of colloidal fluids on to absorbing surfaces such as micro-porous coated papers.

As an ink drop strikes a surface with significant velocity, its subsequent deformation and radial expansion are initially driven by the impact inertia, and later by the drop-surface interaction. For deposition on an absorbent surface, the spreading driven by these forces occurs simultaneously with absorption of the fluid into the surface and with viscous energy dissipation. Accurate prediction of the final shape of a deposited ink drop therefore requires modeling of the imbibition dynamics in addition to the post-impact spreading process. In a study of drop spreading and imbibition on permeable media, Daniel and Berg [9] provided a comprehensive review of the existing modeling work and proposed an energy-based imbibition model. However, their experimental validation did not explore the early, inertia-driven spreading phase. Our aim for this study is therefore not only to characterize the specific deposition behavior of nano-copper ink on to a proprietary micro-porous paper, but also to gain more general insight into the effect of imbibition on the impact and spreading behavior of very small drops deposited by ink-jet printing on permeable surfaces.

2 EXPERIMENTS

The approach of this experimental study was to use high-speed video to capture images of ink drops impacting and spreading on a substrate. These images were then analyzed to extract information about the drop spreading dynamics on surface, specifically the dynamic spreading diameter and the instantaneous drop volume.

2.1 Apparatus and materials

The high-speed imaging apparatus used to study drop deposition was a modified version of that described by Hsiao et al. [11]. In brief, an industrial ink-jet printhead (Xaar 126/80, UK) was used to eject 80 pl ink drops on to a moving substrate. With a constant light source (89 North PhotoFluor II, USA) illuminating the target area from the opposite direction, shadowgraph images of the drops on the substrate surface were captured by a high-speed video

camera (Vision Research Phantom V7.3, USA). The camera was set up to record at 88,888, 10,000, and 5000 fps sequentially in order to capture the complete history of the event from initial impact to drying.

The recorded videos were analyzed with a custom image analysis program, details of which have been described elsewhere [12]. The program converted video frames to binary images using a selectable local threshold value (50% in our analysis) and automatically extracted the shape, width, height and equivalent volume of the deposited drop as a function of the number of captured frames. By taking into account the three different framing rates, these data were then parsed temporally to represent the drop deposition and imbibition dynamics.

Once the profile of the drop became lower than the apparent width of the deposit, the automatic procedure could no longer identify the edges accurately and generally produced spurious results. Images recorded at later times were therefore analyzed manually.

The substrate on which the drop spreading and imbibition behavior were evaluated was a proprietary paper (PEL nanoP60, UK) with a micro-porous top coating. A cross-sectional SEM image and pore size analysis results for the paper are shown in Figure 1.

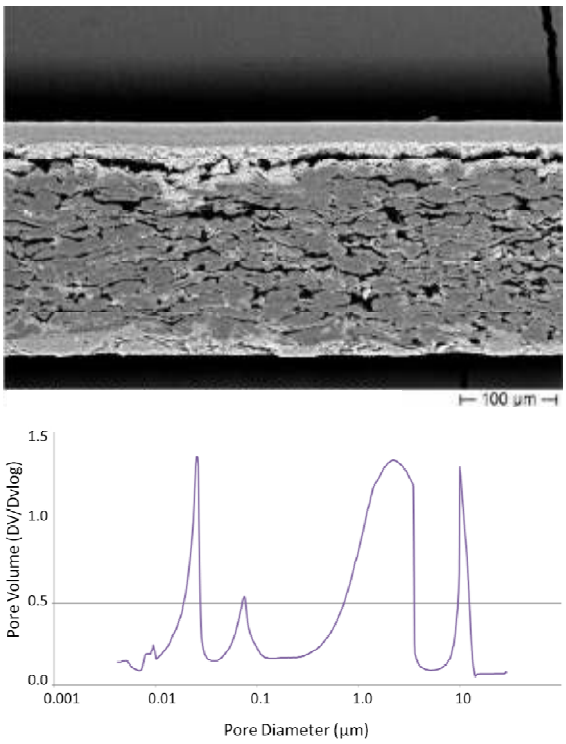

Figure 1: Cross-sectional SEM image and mercury intrusion porosimetry data for the micro-porous paper.

The 23 µm-thick coating was designed to have nanometer scale primary pores, measured to be roughly 25 nm and 70nm in diameter, which matched the particle size of the colloidial ink being deposited. Printing trials with nano-silver inks have shown that functionality (i.e. electrical conductivity) is possible at significantly lower sintering temperature on this substrate than on generic ink-jet photo-papers. However, the reason for the improved performance is not yet fully understood, and this provides additional motivation for an investigation of the ink imbibition process. Ink drops were also deposited on to a generic photo-paper (Fuji photo inkjet paper, 270 gsm) and a non-porous polyimide film as control substrates.

The properties of the nano-copper ink used (Intrinsiq Materials CI002, UK) and the experimental conditions for drop deposition are listed in Table 1. The ink has a primary particle distribution centred at 40 nm. As the ink drops did not reach an equilibrium spherical cap shape on the paper substrates, the associated contact angle values could not be measured. For the polyimide film, the equilibrium static contact angle for the ink, measured from the deposited drop by the spherical fit method, was ~26°.

Conc. (wt%)	ρ (kg/m^3)	σ (mN/m)	µ (Pa.s)	We	Oh
12	1200	40	0.02	6.4	0.4

Table 1: Ink properties (courtesy of Clare Conboy, PEL) and drop deposition condition.

2.2 Results

Typical images of nano-copper ink drops impacting and spreading on the micro-porous paper, photopaper, and polyimide film are shown in Figure 2. With this illumination arrangement, reflections of the impacting and spreading drops are present as mirror images on the substrate surfaces. Up to 33 µs after impact, the initial drop deformation during the kinematic phase was geometrically similar on all three substrates (flattened drop with contact angle greater than 90 degrees). However, the maximum spreading diameter reached at the end of this phase on the non-absorbing polyimide film appears to be larger than that on the papers. In addition, the drop on the polyimide surface undergoes very pronounced contact angle hysteresis, with a transition from the larger advancing to the smaller receding contact angle, in the early relaxation phase between 33 to 55 µs after impact. This hysteresis appears to be more subtle for drops on the absorbent paper surfaces. In fact, the contact angle did not fall below 90 degrees on the papers until 0.5 ms after impact. Beyond 1 ms after impact, the extent of spreading on the papers became more limited than that on the polyimide film. The difference was quite pronounced at 0.1 s after impact and the contact line on the papers became pinned soon after. On the paper substrates, the fluid cap volume reduced progressively with time, whereas the fluid cap diameter began to shrink after only approximately 0.5 s after impact. As the fluid cap shrank, a thin layer of residue was left behind as the contact line receded, giving the deposit a “fried egg” appearance as shown by the images timed at 0.7 s after impact in Figure 2. The cap volume eventually reached zero, or the drop dried completely, at roughly 1.0 s after impact.

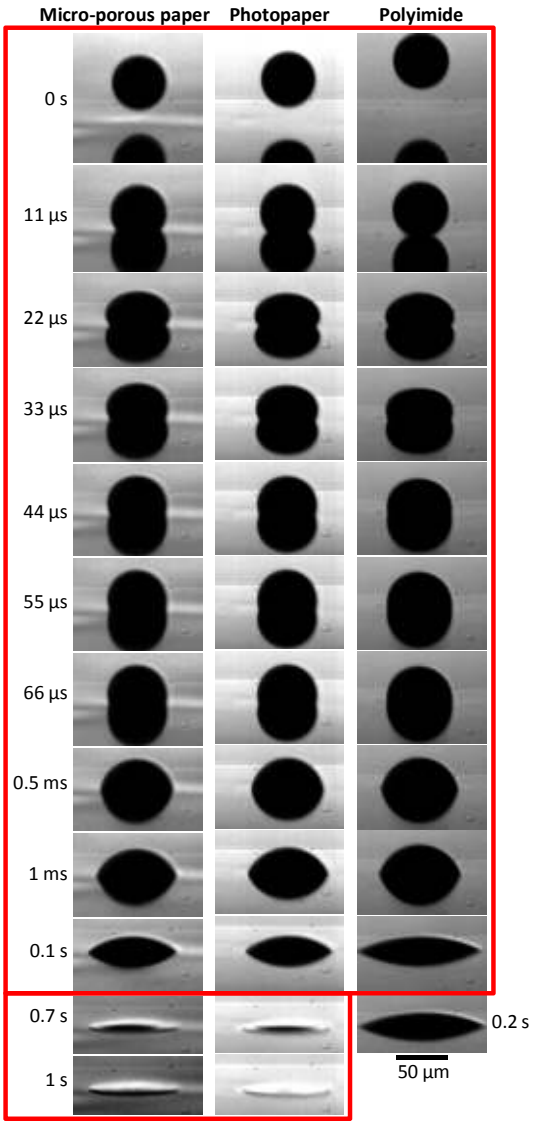

Figure 2: Images of drops of nano-copper ink deposited on to micro-porous paper, photopaper, and polyimide substrates, at the times shown after initial impact.

Quantitative measurements of spreading and imbibition for ink drops on all three substrates are shown in Figure 3. Drop spreading is quantified by the spread factor, $SF = D/D_{ini}$, where D_{ini} is the initial drop diameter and D is the instantaneous width of the contact patch, determined from each pair of images of the drop and its reflection in the substrate. The deposition behavior is plotted in logarithmic time scale to help visualizing the dynamics immediately after impact. The imbibition behavior is represented by the nominal visible volume, $\Phi = v/v_{ini}$, where v_{ini} is the initial drop volume and v is the instantaneous volume of the drop visible on the surface of the substrate. Solid lines for the paper substrates represent the average values for 5 - 6 data sets each. The error bars represent the standard deviations of the data sets.

As expected from images in Figure 2, drops deposited on the micro-porous paper and photopaper showed very similar spreading and imbibition behavior. On both surfaces the deposited drops retracted significantly after the initial, impact-driven spreading. Following that, the drops spread until their contact lines became pinned at around 2 ms after impact. In contrast, on the polyimide surface the drops continued to spread and did not reach equilibrium within the period studied here (100 ms). While the maximum spread diameter after the initial kinematic phase was greater on the polyimide film than on the papers, the spreading rate during the following relaxation and wetting phase was far higher on the papers. This is an unexpected result as qualitative observation of the images in Figure 2 suggested otherwise. The data shows that the smaller spread diameter, and hence the implied slower spreading rate on the paper substrates is really a result of drop contact line pinning at around 2 ms after impact.

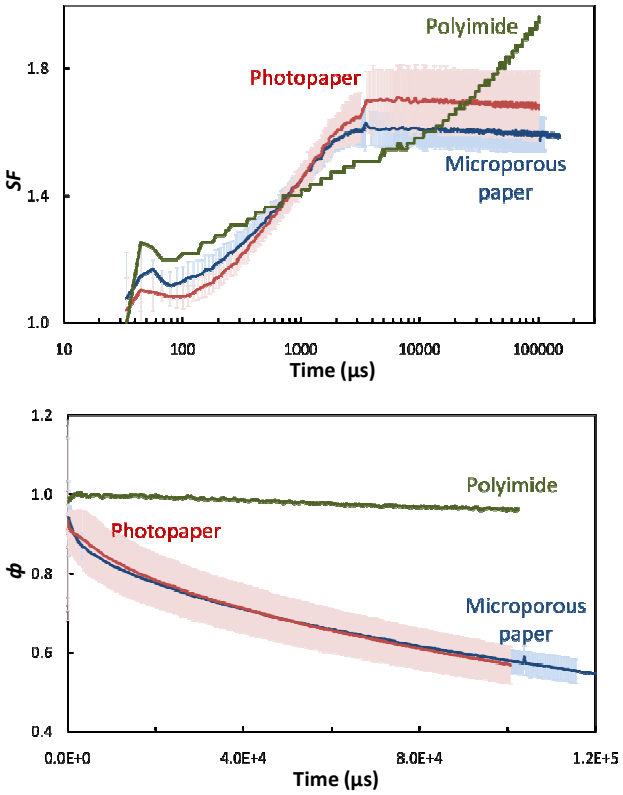

Figure 3: Nano-copper ink drop spreading (top, in logarithmic time scale) and imbibition (bottom) dynamics on micro-porous paper, photopaper, and polyimide.

The similarity between the behaviors on the paper substrates continues in the drop imbibition behavior, as the curves of visible drop volume overlap in the lower plot of Figure 3. As the solvent in the nano-copper ink is moderately volatile, the drop volume loss may be attributed to evaporation as well as imbibition. The extent of evaporation during spreading may be ascertained by the small reduction in drop volume during the later spreading

phase on the non-absorbing polyimide film. The data suggests that volume loss through evaporation is more than an order of magnitude less than the volume reduction observed on the papers. We are therefore confident that imbibition is the dominant factor determining the change in drop volume on the porous surfaces in our experiments.

2.3 Discussion

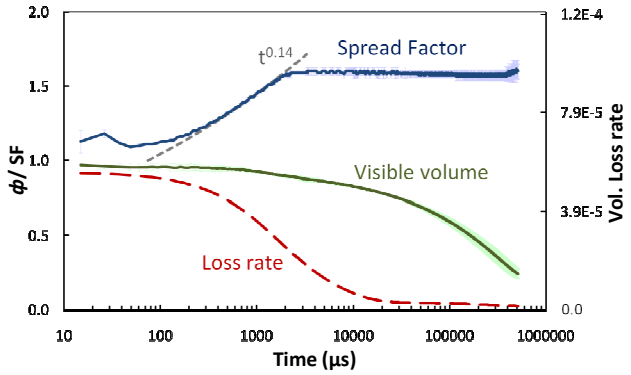

Figure 4: Nano-copper ink drop spreading and imbibition dynamics on micro-porous paper.

The general spreading and imbibition behavior of the nano-copper ink on the micro-porous paper is plotted in logarithmic time scale in Figure 4. The spread factor increases according to a power law with a time exponent of 0.14 from 100 µs to just after 1 ms after impact. The power law correlation is consistent with our earlier results for deposition of UV-curable ink on to a partial-wetting, non-porous metallic surface [11]. However, a specific feature of deposition on to the micro-porous surface is that the spreading terminates decisively when the drop contact line becomes pinned, whereas on the non-absorbing surfaces the contact line tends to continue to move for an extended period of time. Our results therefore suggest that in practice ink-jet dots printed on to porous surfaces such as papers will reach a fixed size within milliseconds after deposition. Such a characteristic will have a significant impact on the coalescence of the printed drops and hence on the quality of the resulting features.

The drop volume loss rate is determined by taking the gradient of an empirical curve fitted to the visible volume as a function of time as:

$$v = Ae^{-\lambda_1 t} + Be^{-\lambda_2 t} + Ce^{-\lambda_3 t} + D \qquad (1)$$

The constants A, B, C and D were chosen to match the initial drop volume (to within 5%), v_{ini}, and the final deposit volume, $D \approx 0.02\ v_{ini}$. The time constants λ_1, λ_2 and λ_3 were adjusted to account for the dynamic shape of the fluid cap over an interval spanning more than 4 orders of magnitude in time (from 15 µs to > 500 ms). The gradient of the function (1), which represents the rate of volume loss, is plotted alongside the curve for the visible volume in Figure 4. It is clear from this plot that the loss rate is not constant over the spreading and drying period. The rate of volume loss, or imbibition rate, appears to diminish from a high value during the kinematic and early relaxation phase to a far lower value (20 to 30 times lower than the earlier rate) towards the end of the drying phase. A potentially significant observation is that the inflection point of the transition from the high to low imbibition rate appears to coincide with the time when the drop contact line is pinned. This clearly suggests a link between contact line motion and imbibition. However, further investigation is required to ascertain the actual mechanism.

3 CONCLUSION

An experimental study has been conducted to characterize the deposition and imbibition dynamics of nano-metallic (copper) ink on to two porous paper substrates. The drop spreading rate is shown to be greater on the papers than on a non-absorbing polymer surface, until the drop contact line becomes pinned. In addition, the ink drop deposited on the papers is shown to cease spreading within milliseconds after impact, significantly shortening the time available for the deposited drops to coalesce and form functional features. Finally, the rate of imbibition on the micro-porous paper varies significantly, with a higher rate immediately after drop impact than during the later drying phase, signifying a potential correlation between the impact inertia and imbibition dynamics.

REFERENCES

[1] A. M Worthington, Proc. R. Soc. London, Ser. A **25**, 261-272, 1876.

[2] S. Chandra and C. T. Avedisian, Proc. R. Soc. London, Ser. A 432, 13-41, 1991.

[3] M. Pasandideh-Fard, Y. M. Qiao, S. Chandra, and J. Mostaghimi, Phys. Fluids **8**, 650-659, 1996.

[4] J. Fukai, M. Tanaka, and O. Miyatake, AlChE J. **31**, 456-461, 1998.

[5] R. Rioboo, M. Marengo, and C. Tropea, Exp. Fluids **33**, 112-124, 2002.

[6] S. H. Davis and L. M. Hocking, Phys. Fluids **11**, 48-57, 1999.

[7] A. Clarke, T. D. Blake, K. Carruthers, and A. Woodward, Langmuir **18**, 2980-2984, 2002.

[8] V. Starov, Adv Colloid Interface Sci **111**, 3-27, 2004.

[9] R. C. Daniel and J. C. Berg, Adv Colloid Interface Sci **123-126**, 439-469, 2006.

[10] H. Dong, W. W. Carr, and D. G. Bucknall, AlChE J. **53**, 2606-2617, 2007.

[11] W.-K. Hsiao, S. D. Hoath, G. D. Martin, and I. M. Hutchings, J. Imaging Sci. Technol. **53**, 050304-050304-8, 2009.

[12] I. M. Hutchings, G. D. Martin, and S. D. Hoath, J. Imaging Sci. Technol. **51**, 438-444, 2007.